



UNIVERSITY
of
GLASGOW

Asenov, A. and Balasubramaniam, R. and Brown, A.R. and Davies, J.H. and Saini, S. (2000) Random telegraph signal amplitudes in sub 100 nm (decanano) MOSFETs: a 3D 'Atomistic' simulation study. In, *International Electron Devices Meeting, 10-13 December 2000*, pages pp. 279-282, San Francisco, California.

<http://eprints.gla.ac.uk/3019/>

Random Telegraph Signal Amplitudes in Sub 100 nm (Decanano) MOSFETs: A 3D 'Atomistic' Simulation Study

A. Asenov[†], R. Balasubramaniam, A. R. Brown, J. H. Davies and S. Saini^{*}

Device Modelling Group, Department of Electronics and Electrical Engineering
University of Glasgow, Glasgow, G12 8LT, United Kingdom

[†] Tel: +44 141 330 5217 Fax: +44 141 330 5236 E-mail: A.Asenov@elec.gla.ac.uk

^{*} NASA Ames Research Center, Moffett Field, CA, 94035, USA

Abstract

In this paper we use 3D simulations to study the amplitudes of random telegraph signals (RTS) associated with the trapping of a single carrier in interface states in the channel of sub 100 nm (decanano) MOSFETs. Both simulations using continuous doping charge and random discrete dopants in the active region of the MOSFETs are presented. We have studied the dependence of the RTS amplitudes on the position of the trapped charge in the channel and on the device design parameters. We have observed a significant increase in the maximum RTS amplitude when discrete random dopants are employed in the simulations.

Introduction

In next generation MOSFETs with sub 100 nm (decanano) dimensions [1], current fluctuations, caused by trapping of single carriers at the Si/SiO₂ interface, and related local modulation in carrier density and/or mobility [2, 3], are becoming increasingly important. Corresponding random telegraph signals (RTS) with amplitudes larger than 60% have been reported already at room temperature in very narrow channel devices [4]. Current fluctuations on such a scale will become a serious issue, not only in analogue circuits, but also in mixed-mode [3] and digital applications. Although the RTS in MOSFETs have been studied experimentally for a relatively long period of time, the developed analytical models [5] and simplified numerical simulation studies [6] can not explain the wide range of RTS amplitudes observed in otherwise identical devices [7]. There are suggestions that due to surface potential fluctuations strategically located traps influence the magnitude and the spreading of RTS amplitudes. However such potential fluctuations have been linked to fixed oxide charges [8] and the impact of the random discrete dopants has not been considered.

In this paper we use 3D 'atomistic' simulations to study the RTS amplitudes associated with trapping/detrapping of single carriers in interface states in the channel of decanano MOSFETs. We investigate the effect of the trapped charge

position and the MOSFET design parameters on the RTS amplitudes, initially employing continuous doping in the simulations. Also, for the first time we illustrate the impact of the discrete random dopants in decanano MOSFETs on both the magnitude and the distribution of the RTS amplitudes.

Simulation approach

The 'atomistic' simulation technique used in this study is described in detail elsewhere [9, 10]. We investigate the change in the drain current associated with trapping of an individual electron in an acceptor type interface state in *n*-channel MOSFETs, assuming continuous or random doping. The simulations are restricted to low drain voltage and do not take into account the local modulation in the mobility associated with the trapped charge.

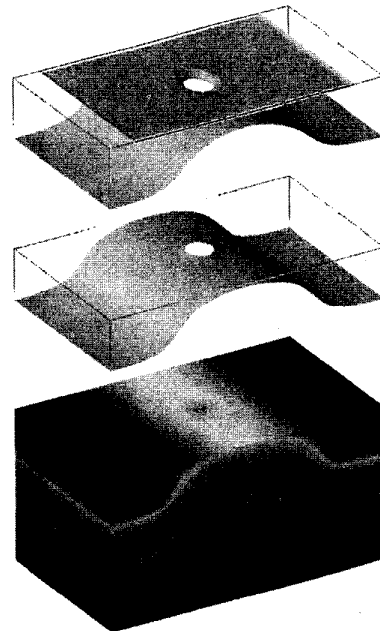


Fig. 1: Potential distribution in a 30x30nm MOSFET with a single trapped electron in the middle of the channel (bottom). An equiconcentration contour is also shown for classical (middle) and quantum mechanical (top) simulations.

12.3.1

The potential distribution in a 30×30 nm *n*-channel MOSFET with continuous doping and one discrete electron trapped exactly in the middle of the channel is presented in Fig. 1. The device is representative for this study having oxide thickness $t_{ox} = 3$ nm, uniform doping concentration in the channel region $N_A = 5 \times 10^{18} \text{ cm}^{-3}$ and junction depth $x_j = 7$ nm with 5 nm lateral sub-diffusion. The equiconcentration contour in the middle of the same figure represents results from classical simulation employing Boltzmann statistics [9]. Quantum corrections using density gradient formalism are incorporated in the solution corresponding to the equiconcentration contour plotted at the top.

Continuous doping simulations

In order to highlight the basic trends and dependencies we first consider continuous doping charge in our 3D simulations. All results presented in this section assume trapping of a single electron at the Si/SiO₂ interface in the middle of the channel, where it has largest influence on the current resulting in maximum RTS amplitudes. The dependence of the corresponding relative RTS amplitudes on the drain current for a set of decanano MOSFETs covering the whole range of device dimensions until the end of the Roadmap is presented in Fig. 2. The effect of the trapped charge is large in the subthreshold region and decreases near and above threshold as a result of the screening by the inversion layer charge. It is noticeable that the maximum RTS amplitude in the 30×30 nm MOSFET reaches more than 40% in the subthreshold region and remains larger than 5% in strong inversion, even assuming continuous doping. The inclusion of quantum corrections in the simulations for the 30×30 nm MOSFET (black dots) produces very little difference and the following results are based on purely classical simulations.

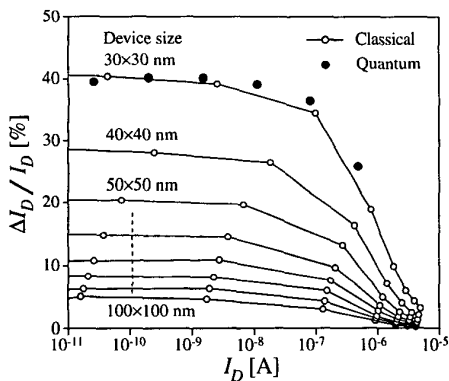


Fig. 2: RTS amplitude ($\Delta I_D/I_D$) dependence on I_D for square devices of different sizes

The trapping of a single electron also results in a threshold voltage shift, illustrated in Fig. 3, which increases more than ten times when the MOSFETs are scaled from 100 to 30 nm.

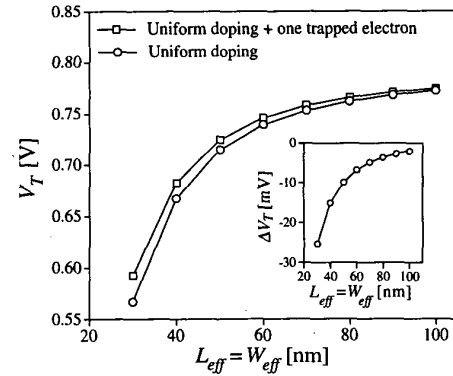


Fig. 3: Comparison of V_T with and without a trapped electron for different sized devices with square geometry. The inset shows the change in V_T associated with the trapped electron. The change is larger than 25 mV for the smallest devices.

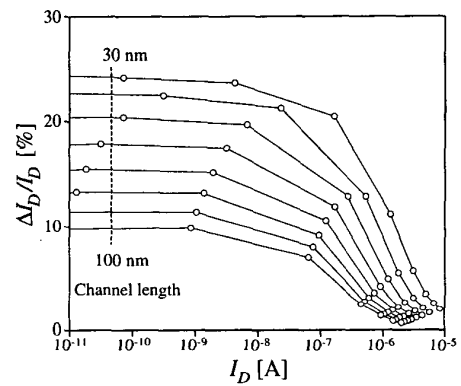


Fig. 4: RTS amplitude dependence on the channel length for a set of devices with channel width 50 nm

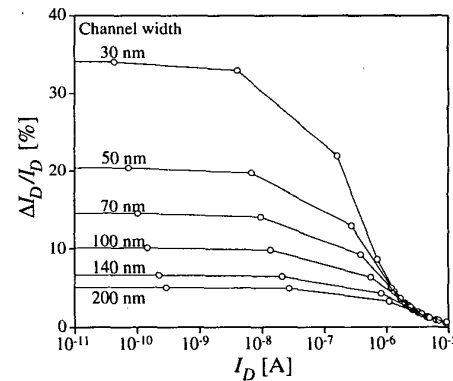


Fig. 5: RTS amplitude dependence on the channel width for a set of devices with channel length 50 nm

12.3.2

The dependence of the RTS amplitudes on the channel length and channel width are illustrated in Fig. 4 and Fig. 5 respectively. Almost linear dependence of the maximum RTS amplitude on the channel length is observed in the subthreshold region in Fig. 4. The threshold voltage roll-off with the reduction of the channel length makes the dependence more complicated near and above threshold. The relative RTS amplitudes on Fig. 5 follow closely $1/\sqrt{W}$ dependence.

Fig. 6 illustrates the influence of the oxide thickness on the RTS amplitudes in 50x50 nm MOSFETs. In the subthreshold region the screening of the Coulomb potential of the trapped electron by the carriers in the gate increases dramatically resulting in a strong reduction of the maximum RTS amplitudes.

Discrete dopants simulations

It has been suggested previously that strategically located traps influence the magnitude and the spreading of the RTS amplitudes due to surface potential fluctuations, and the corresponding current percolation [2, 8], but the potential fluctuations were linked [8] to fixed and trapped interface charge. In properly scaled decanano MOSFETs the random discrete dopants are the major factor, introducing significant surface potential fluctuations and variation in the device parameters even at room temperature [11]. In a 50x50 nm device there are, on average, 170 dopants in the channel depletion region. Their actual number follows a Poisson distribution and their positions are random. The fixed charge has a negligible effect in respect of the potential fluctuations compared to the random dopants. In well controlled technology the surface density of the fixed charge is far below $5 \times 10^{10} \text{ cm}^{-3}$ which is equivalent to approximately one additional discrete charge in every 50x50 nm MOSFET.

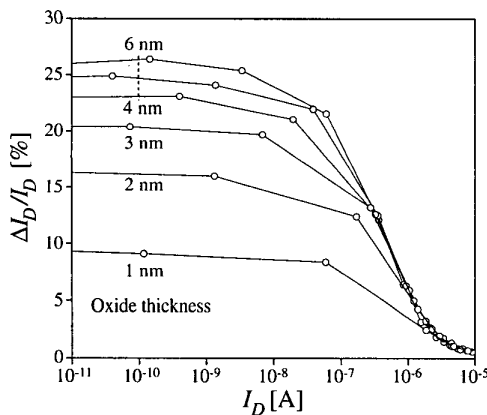


Fig. 6: RTS amplitude dependence on the oxide thickness for a set of 50x50 nm MOSFETs

The potential distribution in the channel of a 50x50 nm MOSFET with discrete random dopants in the channel region is presented in Fig. 7. The current in the presence of random dopants percolates through valleys in the potential landscape. The plane above the channel in Fig. 7 represents (in colour coding) the amplitudes of the RTS fluctuations associated with the trapping of a single electron in an interface state. Unlike the simulations assuming continuous doping, the largest RTS amplitudes in this case (see the RTS magnitude map on top of the potential distribution) are not in the middle of the channel but in the region with the deepest valley in the potential landscape corresponding to the highest density of percolating current.

The drain current dependence of the highest RTS amplitudes in three macroscopically identical but microscopically different 50x50 nm MOSFETs with random doping are compared in Fig. 8. The three random dopant devices are selected from a sample of 200 microscopically different devices to have the largest, the smallest and the middle of the distribution threshold voltages. The maximum RTS amplitudes in the discrete dopant MOSFETs are always higher compared to the continuous doping simulations. The difference is more than three times for the discrete dopant device with the largest threshold voltage. Careful inspection shows that in the device with the lowest threshold voltage ($V_T = 0.49 \text{ V}$) a lucky arrangement of dopants leaves almost half of the channel relatively low doped and highly

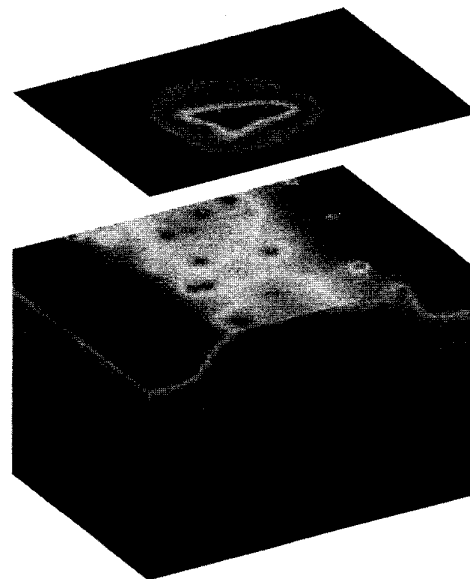


Fig. 7: Potential distribution in a 50x50nm MOSFET with discrete random dopants in the channel region (bottom) and a map of the position dependence of the RTS amplitude for a single electron trapped at the interface (top). The largest RTS amplitude coincides with electron trapping in the region with highest current density.

conductive. The trapping of a single electron there has less dramatic effect compared to the other simulated devices with discrete random dopants. Inspection of the device with the largest threshold voltage ($V_T = 0.85$ V) shows a large concentration of dopants across the middle of the channel leaving very narrow paths for the percolating current. The trapping of a single electron in the vicinity of a dominant but narrow current channel has a dramatic effect on the overall current in this device.

Finally Fig. 9 illustrates the completely different shape of the distributions of the RTS amplitudes in the uniformly doped MOSFET and in the three devices with random dopants. The uniform doping results in a double headed distribution of the RTS relative amplitudes associated with the fact that trapping

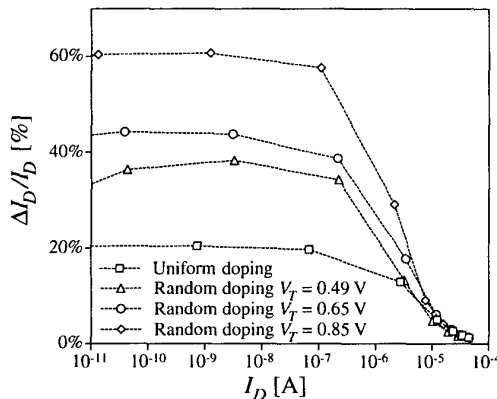


Fig. 8: Highest RTS amplitudes for 3 50×50 nm devices with different atomic doping, and one with uniform doping, with a single electron trapped in the worst-case location

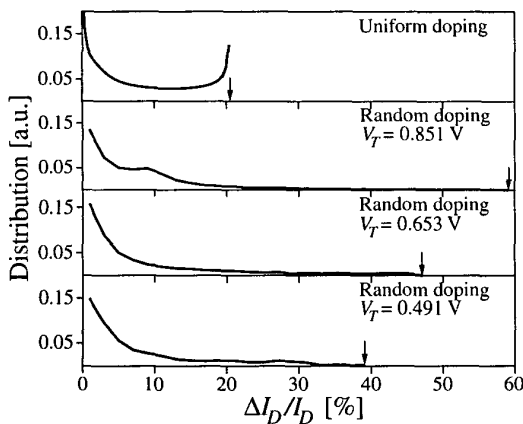


Fig. 9: Distribution of RTS amplitudes for the 4 devices from Fig. 8

in the middle of the channel produces large amplitudes and trapping near the source and the drain have a negligible effect.

In the discrete dopant case the low-amplitude part of the distribution is similar in shape to the continuous dopant case because near the source and the drain the dopant fluctuations are less effective due to the built-in junction potential. However the high-amplitude part of the distribution extends to much larger amplitudes and the bumps and nonuniformity of the distribution represent the complex current percolation patterns in the individual devices.

Conclusions

Trapping and detrapping of a single charge will have a dramatic effect on the operation of decanano MOSFETs near the end of the Silicon Roadmap. The relative RTS amplitudes will reach the order of several tens of percent when below threshold, reducing to a few percent when above threshold, in devices with a square geometry. This estimate is based on the local modulation of the conducting charge in the channel and does not include the effect of the trapped charge on the channel mobility.

We have also demonstrated that the random dopant induced surface potential fluctuations and the associated current filamentation are responsible for a significant increase in the RTS amplitudes compared to the results of simulations which assume a continuous doping distribution. The use of realistic random dopant distributions in the simulations also modifies the distribution of the RTS amplitudes in an ensemble of macroscopically identical devices.

References

- [1] International Technology Roadmap for Semiconductors, 1999 Edition.
- [2] K.S. Rals, W.L. Skokpol, L.D. Jakel, R.E. Howard, L.A. Fetter, R.W. Epworth, and D.M. Tennant, Phys. Rev. Lett., 63, 228, 1984
- [3] S.T. Martin, G.P. Li, E. Worley, and J. White, IEEE Electron Device Letters, 18, 444, 1997
- [4] Y. Shi, H.M. Bu, X.L. Yuan, and Y.D. Zheng, in Workshop Abstracts, Silicon Nanoelectronics Workshop, Kyoto, 1999
- [5] E. Simoen, B. Dierick, C.L. Claeys, and G.J. Declerck, IEEE Trans. Electron Devices, 39, 422, 1992
- [6] A. Godoy, F. Gamiz, A. Palma, J.A. Jimenez-Tejada and J. Banqueri, J. Appl. Phys., 82, 4621, 1997
- [7] M.-H. Tsai and T.-P. Ma, IEEE Trans. Electron Devices, 41, 2061, 1994
- [8] M.J. Uren, D.J. Day and M.J. Kirton, Appl. Phys. Lett., 47, 1195, 1985
- [9] A. Asenov, A. R. Brown, J. H. Davies and S. Saini, IEEE Trans. on CAD of Integrated Circuits and Systems, 18, 1558, 1999
- [10] A. Asenov, G. Slavcheva, A. R. Brown, J. H. Davies and S. Saini, Proc. IEDM'99, Dig. Tech. Papers, pp.535-538
- [11] A. Asenov, IEEE Trans. Electron Devices, 45, 2505, 1998